

How cryptic is cryptic diversity? Machine learning
approaches to classifying morphological variation in
Emys marmorata (Testudinoidea, Emydidae).

Peter D Smits¹, Kenneth D Angielczyk^{1,2}, and James F Parham³

¹Committee on Evolutionary Biology, University of Chicago

²Integrative Research Center, Field Museum of Natural History

³Department of Geological Sciences, California State University – Fullerton

August 9, 2013

Corresponding author: Peter D Smits, Committee on Evolutionary Biology, University of Chicago, 1025 E. 57th Street, Culver Hall 402, Chicago, IL, 60637, USA; E-mail: psmits@uchicago.edu

Abstract

2 Cryptic diversity is the phenomenon where some taxa are believed to be identifiable
only based on molecular data. This is concerning because the majority of extant taxa
4 and virtually all extinct taxa are delimited entirely via morphology. Here we address
questions about whether it is possible to determine, based on morphology, if one
6 classification hypotheses can be considered better than others. Using a combination

of unsupervised and supervised machine learning methods we demonstrate a suite of approaches for better understanding differences in morphology between classes, the odds of classifying one class relative to another, and what aspects of morphology best describe the differences between classes. These approaches are applied to the classification of the emydid turtle, *Emys marmorata*. This species has conflicting hypotheses of the number of meaningful subclades based on either morphological or molecular information. We compared multiple explicit classification hypotheses by characterizing variation in plastral shape and how it may be identifiably different between different classes. By splitting a large dataset of specimens into both training and testing datasets, we were also able to determine which of the classification hypotheses best corresponded to the observed plastral variation. The results from our analysis shows that the best classification of plastral variation in *Emys marmorata* is in accordance with the molecularly based hypothesis. This demonstrates that, by using alternative methods for characterizing variability, it is possible to estimate the classification scheme which most agrees with observed morphological variation. Additionally, we demonstrate that it is possible that not all examples of cryptic variation may be truly cryptic, just a product of sample size or methodology because of the extremely fine scale variation between the different classes.

(Keywords: Testudines, Emydidae, morphology, geometric morphometrics, random forests)

Cryptic diversity is the phenomenon that not all taxa can be recognized based on morphology and can only be delimited using molecular information (Clare 2011; Funk et al. 2012; Pfenninger and Schwenk 2007; Stuart et al. 2006). Conceringly, most extant taxa, and nearly all extinct taxa, are delimited based solely via morphological analysis. This phenomenon is of great concern when studying variation and diversity dynamics over long periods of time, where apparent morphological stasis may not actually reflect true diversity (Eldredge and Gould 1972; Gould and Eldredge 1977; Hunt 2008). In the case of

34 endangered or conserved taxa, morphometric approaches for classifying and identifying taxa
and populations of importance would greatly improve the ability to maintain these high risk
36 groups. Additionally, this would allow for better classifying extinct taxa.

Much work has been devoted to species delimitation via sequence difference (Fujita
38 et al. 2012; Yang and Rannala 2010) while comparatively little has been devoted to introducing
new methodology for case of purely morphological data (Mitteroecker and Bookstein 2011;
40 Zelditch et al. 2004). The majority of this effort has focused on identifying differences between
already identified taxa (Demandt and Bergek 2009; Gaubert et al. 2005; Gündüz et al. 2007;
42 Polly 2003, 2007; Zelditch et al. 2004) and automated taxon identification (MacLeod 2007).

Here, we address the question of how can alternative approaches and methodology
44 improve morphology based classification. From this approach, we ask if it is possible to
determine which amongst a set of classification hypotheses is best.

46 *Background and system*

Differences in morphological variation between different classes has previously been analyzed
48 using methods like linear discriminate analysis and canonical variates analysis (Demandt
and Bergek 2009; Gaubert et al. 2005; Gündüz et al. 2007; Mitteroecker and Bookstein 2011;
50 Polly 2003, 2007; Zelditch et al. 2004). These methods are comparatively simple and straight
forward ways of understanding the differences in morphology between classes. Also, they are
52 very visual methods which aides in interpretation and presentation of information. These
previous studies, however, do not compare which amongst a set of candidate classification
54 hypotheses is better. For example, studies such as those of Caumul and Polly (2005) and
Polly (2007) focused on comparing different aspects of morphology and their fidelity to a
56 classification scheme, instead of comparing the fidelity of one aspect of morphology to multiple
classification shcemes. Also, there is no generalization of the classification model and training
58 data accuracy is almost exclusively used as the metric off strength of classification.

Here, we used multiple machine learning methods, both unsupervised and supervised,
in order to compare different classification hypotheses. These methods provide different and
unique advantages for understanding how to classify taxa, with what accuracy, and what these
classifications are based on. While machine learning methods such as neural networks have
been applied to studying shape variation (MacLeod 2007), they have been primarily applied
in the context of automated taxon identification and not in terms of group classification
and strength of classification. Additionally, we investigate variation in continuous traits, and
do not search for discrete differences between each class, instead focusing on multivariate
quantification of shape.

The two major classes of machine learning methods, unsupervised and supervised,
are essentially extensions of known statistical methods (Hastie et al. 2009). Unsupervised
learning methods are analogous to clustering and density estimation methods (Kaufman
and Rousseeuw 1990), while supervised learning methods are analogous classification and
regression models (Breiman et al. 1984). In both cases, many of these methods are not fit
via maximum likelihood and are supplemented by randomization, sorting, and partitioning
algorithms along with the maximization or minimization of summary statistics in order
to best estimate a general model for all data, both sampled and unsampled (Hastie et al.
2009). The application of the alternative approaches used in this study illustrates only a
sampling of the various previously derived methods for clustering observations and fitting
classification models. Additionally, instead of pure classification accuracy, here we use a
statistic of classification strength that reflects the rate at which taxa are both accurately and
inaccurately classified (see Methods).

In this study, we investigate the subspecific classification of the western pond turtle,
Emys marmorata. *E. marmorata* is distributed from northern Washington State, USA
to Baja California, Mexico. Traditionally, *E. marmorata* was classified into three groups:
the northern *E. marmorata marmorata*, the southern *E. marmorata palida*, and a central

Californian intergrade zone (Seeliger 1945). *E. marmorata marmorata* is differentiated from
86 *E. marmorata palida* by the presence of a pair of triangular inguinal plates and darker neck
markings. It should be noted that the triangular inguinal plates can sometimes be present in
88 *E. marmorata palida* though they are considerably smaller.

Previous work on morphological differentiation in *E. marmorata* focused on compar-
90 isons between different populations within the range CITATIONS. Most of these studies were
not over the entire range and used only linear measures of morphology instead of multivariate
92 shape CITATIONS. Holland (1992) used comparisons of linear measures of the carapace of
E. marmorata from different populations over the entire range of the species. This study
94 was interested in the relative effect of distance versus barriers had in terms of fostering
morphological differentiation in *E. marmorata*. Analyses were performed to determine how
96 different, morphologically, different populations in three different regions of the species range.
Additionally, sexual dimorphism present in *E. marmorata* was only assessed in the context of
98 size measures such as length of carapace and mass. In general, Holland (1992) and others
(Germano and Rathbun 2008; Lubcke and Wilson 2007) found that males of *E. marmorata* are
100 larger than females in terms of size. However, the effect of sexual dimorphism on shape, *sensu*
Kendall (1977) and Dryden and Mardia (1998), was not assessed (Germano and Rathbun
102 2008; Holland 1992; Lubcke and Wilson 2007).

Holland (1992) concluded that distance was a poor indicator of morphological differen-
104 tiation as opposed to barriers, such as different drainage basins, are probably more important
barriers to reproduction. This conclusion was later echoed by Spinks and Shaffer (2005) via
106 molecular phylogenetic analysis. Additionally, Holland (1992) found that with increasing
amount of barriers and distance, morphological differentiation was observable though the
108 underlying variation required many variables obtain indicating the very fine degree of mor-
phological differentiation between putatively distinct populations. Holland (1992) concluded
110 that *E. marmorata* is best classified as three distinct species as opposed to subspecies: a

northern species, southern species, and Columbia basin species. This classification is similar
112 to Seeliger (1945), except elevated to the species as opposed to subspecific level.

More recently, *E. marmorata* was divided into four clades based on mitochondrial
114 DNA: a northern clade, a southern clade, and eastern and western central Californian clades
(Spinks and Shaffer 2005; Spinks et al. 2010). While nuclear DNA supports two major clades,
116 one northern and one southern, Spinks et al. (2010) argue that the four clade classification is
of greater conservation utility. While the mitochondrially based classification is considered
118 robust, there is no known morphological differentiation between these clades.

In this study, we attempt to estimate the best classification scheme of *E. marmorata*
120 based on variation in plastral shape. Because of unclear geographic boundaries between
subgroups of *E. marmorata*, we compare two hypotheses of morphologically based classification
122 and two hypotheses of molecularly based classification. We hypothesize that if morphological
variation corresponds to class assignment, then it should be possible to determine the best
124 classification hypothesis of *E. marmorata* from amongst multiple candidate hypotheses.
However, if morphological variation does not correspond to any classification
126 hypothesis, then supervised learning model generalization performance will be poor and
reflect how variation may not follow along with any of the candidate classification hypotheses.

128 MATERIALS AND METHODS

Specimens

130 We collected landmark-based morphometric data from 524 adult *E. marmorata* museum
specimens. These specimens include both newly sampled individuals and those sampled in
132 previous studies of plastral shape variation (Angielczyk and Feldman 2013; Angielczyk et al.
2011; Angielczyk and Sheets 2007). Specimen classification was based on known specimen

geographic information which was recorded from museum collection information. When precise latitude and longitude information was not available it was estimated from whatever locality information was present. Because the specimens used to define the subclades in Spinks and Shaffer (2005) and Spinks et al. (2010) were not available for study, all specimen classifications were based solely on this geographic information and not from explicit assignment in previous studies. The classifications here were based on matching museum locality data with the geographic boundaries of the molecularly-defined clades of Spinks and Shaffer (2005) and Spinks et al. (2010). Because the exact barriers between different biogeographic regions are unknown and unclear, two assignments for both the morphologically and molecularly based hypotheses were used. Each morphologically based hypothesis had three classes, while each molecular-based had four classes. In total, each specimen was given four different classifications.

Geometric morphometrics

Following previous work on plastral variation (Angielczyk and Feldman 2013; Angielczyk et al. 2011; Angielczyk and Sheets 2007), 19 landmarks were digitized using TpsDig 2.04 (Rohlf 2005). These landmarks were chosen to maximize the description of general plastral variation (Fig. 1). 17 of these landmarks are at the endpoints or intersection of the keratinous plastral scutes that cover the plastron. 12 of these landmarks were chosen to be symmetrical across the axis of symmetry and, in order to prevent degrees of freedom and other concerns (Klingenberg et al. 2002), prior to analysis these landmarks were reflected across the axis of symmetry (i.e. midline) and the average position of each symmetrical pair was used. In cases where damage or incompleteness prevented symmetric landmarks from being determined, only the single member of the pair was used. Analysis was conducted on the resulting “half” plastra. Plastral landmark configurations were superimposed using generalized Procrustes analysis (Dryden and Mardia 1998) after which, the principal components (PC) of shape

were calculated. This was done using the `shapes` package for R (Dryden 2013; R Core Team
160 2013).

Machine learning analyses

162 *Unsupervised learning.*— In order to preserve the relationship between all landmark configura-
rations in shape space, the dissimilarity between observations was measured using Kendall’s
164 Riemannian shape distance or ρ (Dryden and Mardia 1998; Kendall 1984). This metric
was chosen because shape space, or the set of all possible shape configurations following
166 Procrustes superimposition, is a Riemannian manifold and thus non-Euclidean (Dryden and
Mardia 1998). ρ varies between 0 and $\pi/2$ when there is no reflection invariance, which should
168 not be a concern in the case of the half plastral landmark configurations used in the study.

The ρ dissimilarity matrix was divisively clustered using partitioning around mediods
170 clustering (PAM), a method similar to k -means clustering except that instead of minimizing
the sum of squared Euclidean distances between observations and centroids, the sum of squared
172 dissimilarities between observations and mediods is minimized (Kaufman and Rousseeuw
1990). Because the optimal number of clusters of shape configurations in the study was
174 unknown, being possibly three, four, or some other value, clustering solutions were estimated
with the number of clusters varied between one and 40. Clustering solutions were compared
176 using the gap statistic, which is a measure of goodness of clustering (Tibshirani et al. 2001).
The gap statistic is defined

$$Gap_n(k) = E_n^*[\log(W_k)] - \log(W_k)$$

178 where W_k is

$$W_k = \sum_{r=1}^k \frac{1}{2n_r} \left(\sum_{i,i' \in C_r} d_{ii'} \right)$$

. $d_{ii'}$ is the dispersion of the clustering solution or the sum of the pairwise dissimilarities between observations in each cluster and their respective medoids (C) for all clusters r . This value is averaged and compared to the expected dispersion (E_n^*) of a sample n from a reference distribution. In this case, the reference distribution was estimated from 500 resamples of the dataset while maintaining the original dispersion of the data. This analysis was conducted using the `cluster` package for R (Maechler et al. 2013) using all 524 observations.

Supervised learning.— The total dataset of 524 observations was split into training and testing datasets. The training dataset represented 75% of the total dataset, split proportionally by class, and was used for model fitting. The testing dataset represented the remaining 25% of the total dataset and was used after model fitting to estimate the effectiveness of each classification hypothesis and generalizability of the supervised learning models (i.e. performance in the wild). This split was chosen to allow for a large enough sample size for model fitting while also providing a large enough testing dataset to determine any systematic misclassifications.

Three different supervised learning methods were used to model the relationship between plastral shape and class: linear discriminate analysis, multinomial logistic regression and random forest. These methods were chosen because of various properties of these methods which allow for useful interpretations about the quality and structure of the classification.

Linear discriminate analysis (LDA) is a frequently applied method for characterizing the primary differences in morphology between different classes (Mitteroecker and Bookstein 2011; Zelditch et al. 2004). This method attempts to find a linear combination of predictors to best model two or more classes. LDA is very similar to PCA except that instead of finding the linear combination of features that maximize the amount of explained variance in the data, LDA maximizes the differences between classes. The results of this analysis produces a transformation matrix by which the original features can be transformed to reflect the best

discrimination between the classes. Like other supervised learning methods, LDA can also be used for predictive analysis on testing data. LDA was done using the **MASS** package for R (Venables and Ripley 2002).

Multinomial logistic regression is an extension of logistic regression, where instead of a binary response there are three or more response classes (Venables and Ripley 2002). Effectively, this type of model can be viewed as multiple, simultaneous logistic regression models for each class and the final classification of the observation being the most probable of all the constituent model results. Similar to the odds ratios calculated from the coefficients of a logistic regression, the relative risk of a classification with reference to a baseline class can be determined from the coefficients of the model. Multinomial logistic regression models were fit using the **nnet** package for R (Venables and Ripley 2002)

Random forest models are an extension of classification and regression trees (CART) (Breiman 2001; Breiman et al. 1984). Because this study relies on classification models, CARTs are explained with reference to classification but the approach is equally valid for regression. The goal of CARTs are to use a series of different features to estimate the final class. In top-down induction of decision trees for each member of a given set of predictor variables, attribute value test are used to estimate the differences between classes. This process is then repeated on each subset, called recursive partitioning. The recursion continues until the resulting observations all share the same class or no more meaningful partitions are possible. The resulting model is a tree structure by which observations are classified at each intersection via the estimated cutoff points from the attribute tests made during model fitting.

In a random forest model, many CARTs are built from a random subsample of both the features and the observations. This process is then repeated many times and the parameters of the final model was chosen as the mode of estimates from the distribution of CARTs (Breiman 2001). In addition to fitting a classification model, this procedure allows for the

features to be ranked in order of importance. In the context of this study, this means that the PCs most important for describing the difference between classes can be estimated, and thus illustrate the most important variation amongst classes as opposed to just the greatest amount of variation in the entire dataset. This is a generally important property that is useful for many other studies which want to describe and model the differences between classes and the relative importance different features. Random forest models were fit using the `randomForest` package for R (Liaw and Wiener 2002).

The supervised learning models used here, except LDA, have tuning parameters which help to increase the generalizability of the model and prevent them from being overfit. For the supervised learning models fit in this study, tuning parameters were estimated via 10 rounds of 10-fold cross-validation (CV) across a grid search of all tuning parameter combinations. Optimal tuning parameter values were selected based on area under the receiver operating characteristic (ROC) curve. The area under the multiclass ROC curves was estimated using the all-against one strategy derived by Hand and Till (2001). This tuning process was implemented following the default grid search implemented in the `caret` package for R (Kuhn 2013).

ROC is a confusion matrix (Table 1) statistic that is a descriptor the relationship between the false positive rate (FPR , Eq. 1) of a classification model and the true positive rate (TPR , Eq. 2) of a classification model (Hastie et al. 2009). The area under the ROC curve (AUC) is a summary statistic of the quality of the classification and varies between 0.5 and 1, with values of 0.5 indicating a model that classifies no better than random and a value of 1 indicating perfect classification (Hastie et al. 2009). AUC can be used as a model selection criterion for classification models and is especially useful in cases where some if not all of the models in question were not fit via maximum likelihood where a criterion such as AICc (see below) or similar can be used (Hastie et al. 2009). It is important to note that, unlike AICc, AUC is not calculated with reference to the complexity of the model.

$$FPR = \frac{FP}{FP + TN} \quad (1)$$

$$TPR = \frac{TP}{TP + FN} \quad (2)$$

Normally, LDA is applied to the entire set of eigenscores from the PCA of shape (Mitteroecker and Bookstein 2011). Instead here LDA was applied on the eigenscores from a subset of the total number of PCs, ranging from two to 10 in increasing order of complexity. In total, this produced nine different LDA scaling matrices. From this set, the best number of PCs used to determine the LDA scaling matrix were chosen. As LDA is “fit” via maximum likelihood, the final combination of number of PCs and LDA scaling matrix chosen was that with the greatest AUC value from the training set.

For the multinomial logistic regression models, 10 different models were fit each having sequentially more PCs as predictors in order to have models representing different levels of overall amount of shape variation and to estimate how much was necessary and sufficient to best estimate class. The maximum number of PCs allowed as predictors was 10 because of both the large number of parameters estimated per model and the necessary sample size needed to estimate that many parameters accurately. The final model was that with the lowest AICc (Akaike 1974; Burnham and Anderson 2002; Hurvich and Tsai 1989). AICc is a model selection criterion where the model with lowest AICc has the fairest variance–bias tradeoff (Burnham and Anderson 2002). Model selection was performed in this manner because the optimal number of PCs to use as predictors was not known *a priori*, and while including all of the PCs of shape would mean that all shape variability would be used to estimate class, this may cause the model to be overfit and not provide an accurate estimate of unsampled plastral variation. In addition to the AICc of each model the $\Delta AICc$ and Akaike weights are also reported. $\Delta AICc$ values are the difference in AICc between the AICc best model and that model while Akaike weights are a transformation of the AICc of a model with relation to all

other models being compared and measures the relative amount of information explained by
that model compared to all other models (Burnham and Anderson 2002).

Random forest models are not fit using maximum likelihood so AICc based model
selection was not possible. Instead, a recursive feature selection algorithm was used to choose
the optimal number of PCs to include based on the AUC of the model. Following the
backwards selection algorithm implemented in `caret` (Kuhn 2013), the maximum number of
features were included in the initial model, their importance ranked, and the AUC of the
model calculated. The lowest ranked feature was then removed, and the AUC of the model
recalculated. This was repeated until only one feature, remained. Similar to the multinomial
logistic regression models described above, the maximum number of PCs that could have
been included in the model was 10. After each PC was removed , 10-fold CV was used to
estimate the optimal values of the tuning parameters as well as quantify the uncertainty of
each model. Random forest model parameters were estimated from 1000 subtrees. Because
PCs were kept in order of importance and not in relation to the amount of variance each PC
described, this means that the exact PCs included in each model do not correspond to the
PCs in each of the 10 multinomial logistic regressions models.

The final selected models were then used to estimate the class assignments of the
training dataset. Model generality for both methods for all four classification schemes was
measured using the AUC of the assignments. A distribution of AUC values was estimated
for each classification scheme via 1000 nonparametric bootstrap resamples of the training
dataset. The difference in distributions was assessed using pairwise Mann-Whitney U tests.

RESULTS

Geometric morphometrics

302 The results of the PCA of the total dataset of *E. marmorata* pastral landmarks configurations
demonstrates no clear or obvious groupings (Fig. 2). The first three PCs, which represent
304 45.29% of the total variation, are a cloud of points with no structure. Additionally, individual
landmark variation is mostly circular around each landmark with some more elliptical
306 variation observed along some midline landmarks and the most lateral landmark (Fig. 2).
However, it is important to note that Procrustes based superimposition attempts to evenly
308 distribute variance around the mean shape (Zelditch et al. 2004) and this observation should
be considered cursory at best.

310 The first two PCs appear to describe principally variation in the lateral margin of the
palstra, from a pointed medial edge to a more rounded and blunt edge (Fig. 3). Landmark 10
312 (Fig. 1), which appears to be the most variable along these axes (Fig. 2 and 3), is positioned
on the bridge between the plastron and the carapace. Over ontogeny, this is an area that
314 deepens dorsoventrally and when the plastron was projected into two dimensions this it
created the effect of mediolateral movement. Lateral landmark variation along the first PC
316 seemed concentrated in the posterior portion of the plastra with additional variance observed
in midline landmarks (Fig. 3). This variance in midline landmarks was most likely caused by
318 the fact that pastral scutes frequently do not line up perfectly. Along PC 2, lateral variation
appeared to be concentrated in the anterior portion of the plastra (Fig. 3).

320 *Machine learning analyses*

Unsupervised learning.—

322 Comparison of gap statistic values for the range of PAM solutions indicates that the
optimal number of clusters is one (Fig. 4). The next best clustering solution had only two
324 clusters, however there is no geographic structure to this classification scheme, with members
of these clusters being seemingly randomly distributed (Fig. 5). Importantly, these clusters do

not conform to the northern and southern groups from the nuclear DNA hypothesis (Spinks et al. 2010).

Sex information was only available for 399 of the 524 turtles. A χ^2 test of the relationship between sex observation and cluster assignment from PAM with two clusters showed that there was no significant relationship between cluster assignment and sex observation (χ^2 : 1.12, df: 1, p -value: 0.29, Table 2). This results is interesting because while sexual dimorphism has been observed in linear measures and mass estimates of *E. marmorata*, this results demonstrates that this dimorphism may not translate into differences in shape. Interestingly, male emydid turtles are known to have a plastral concavity which may influence landmark position along the midline. However, the plastral concavity of *E. marmorata* males is considered less pronounced than in other emydid turtles.

The gap statistic values for both three and four clusters are much lower than for one and two and are statistically identical. Interestingly, other solutions with a much greater number of clusters have higher gap statistic values though these are also not significantly different. Increasing the number of clusters does appear to improve the gap statistic enough compared to the best clustering solution to merit detailed discussion.

Supervised learning.—

The optimal number of PCs used for LDA, as determined by highest ROC score, for three of the four classification schemes had all 10 possible PCs (Fig. 6). These were both of the morphological based classification hypotheses and the second molecular hypothesis. LDA of the PCs of the first molecular hypothesis found that, based on ROC, only the first 9 PCs were necessary to best discriminate between the classes (Fig. 6).

The AICc best multinomial logistic regression model for three of the four classification schemes had the first 9 PCs as features (Tables 3, 4, and 5). The second molecularly based classification hypothesis included all 10 possible PCs as predictors (Tables 6). The Δ AICc

values between the optimal and second best model range from 1.18 for the first morphological
based classification hypothesis to 26.51 for the second molecular based classification hypothesis
(Tables 3, 4, 5, and 6). The first 9 PCs describe 83.23% of total variation in plastral shape,
while the first 10 PCs describe 86.54% of the variation.

While the ΔAICc value between the optimal and second best model for the first
morphological and first molecular based classification hypothesis was within the range to
be considered equally optimal (Burnham and Anderson 2002), for this analysis we chose to
use only the AICc best model. While AICc values can not be compared between models
with different responses (Burnham and Anderson 2002), we interpret the fact that the
 ΔAICc best model in these cases is the simpler model and that the optimal model for
three of the classification schemes having the same number of predictors as reasons to use
only the AICc best model for all cases. Additionally, by using a single model for each of
the classification hypotheses, this limits the number of comparisons between the bootstrap
resampled distributions of the AUC values for the testing dataset (see below).

The selected number of features in the final random forest model for each classification
scheme was very similar to the model selection results from the multinomial logistic regression
models, ranging from 9 for the second morphological based classification hypothesis and both
molecular based classification hypotheses to 10 for the first morphological based classification
hypothesis (Fig. 6).

In the case of all models, there is a substantial increase in model performance as
measured by AICc for the multinomial logistic models (Tables 3, 4, 5, and 6) or in AUC for
the LDA-based predictions and random forest models and illustrated for the multinomial
logistic regression models as the number of features increases (Fig. 6).

The results from the generalization of the selected supervised learning models, mea-
sured by the distributions of the bootstrapped AUC values of the testing dataset, show
that a molecular classification hypotheses was the best overall classification scheme (Fig.

7). Remarkably, the best classification hypothesis was the second molecular classification hypothesis based on the LDA-based predictions, the multinomial logistic regression and random forest models. For both methods, the distribution of bootstrapped AUC for the molecular hypothesis was significantly greater than all of the other classification schemes (Tables 9, 7 and 8).

When the classification results of the training set for the best classification scheme based on the generalization results are compared with the reference classes, the higher AUC value of the best results from LDA and the best multinomial logistic regression model compared to the best random forest model can be observed as the classifications are much closer to the reference classes (Fig. 8). The best random forest model misclassified many of the observations as the northern clade instead of the correct class. This pattern of misclassification is observable but not as exaggerated in the classifications of the multinomial logistic regression model.

This pattern of misclassification may have been caused by the subtle differences in mean shape between each of the different classes (Fig. 9). The mean shape of the northern clade is the most similar to the mean shape of the entire dataset (Fig. 9a), which may indicate that specimens that are closer to the mean shape will be systematically misclassified as the northern clade.

The results of fitting the final random forest model also include the variable importance for best separating the different classes. The selected random forest model for the best classification scheme had 9 PCs as features. The PCs included as features in the final random forest model, in descending order of importance, were PCs 3, 2, 1, 6, 5, 10, 9, 8 and 4. Of these 9 features, the first three are illustrated here (Fig. 10) in descending order of importance.

The first two most important features describe different aspects of variation (Fig. 11). The third and most important PC describes variation roundedness of the medial portion of the plastron, both the anterior and posterior portions of the plastron. Additionally, the relative

position of the landmarks along the midline varies greatly along PC3 (Fig. 11). This PC
404 represents 12.19% of total variation. The second and second most important PC is described
above and principally described variation in landmarks along the lateral and anterior margin
406 of the plastron. This PC represents 12.78% of total variation. The major variations along
these axes correspond well to the differences between the mean shape of each class (Fig.
408 9) where major class differences seem based on the relative ballooning or shrinking of the
anterior and posterior portions of the plastron together along with differential “pinching” of
410 the midline landmarks.

The relative risk values for classification from the multinomial logistic regression
412 model, based on the three most important PCs, demonstrate that individual axes contribute
to classification differently and that given multiple features the odds of determining the
414 correct classification increase (Fig. 12). The first most important axis contributes strongly
to classifying both the western and southern groups while changes along the second most
416 important axes contribute very little to increasing the odds of classification for all but the
eastern group. This is observable from the class histograms of PC 3 and 2 (Fig. 11). Changes
418 along the first and third most important axes contribute more obviously to increasing the
odds of correctly identifying the class of an observation, a result that is observable in both
420 the relative risk (Fig. 12) and the different class histograms of the PCs (Fig. 11).

The graphical results from the LDA of the training dataset for models of the second
422 molecular classification scheme agree with the subtle distinctions between the different classes
(Fig. 13). There is no clear distinction in terms of multivariate space between the four different
424 classes. Instead, across all three axes there is substantial overlap as indicated by both the
scatter of the points in space and the distribution of observations along each axis.

426 DISCUSSION

The results of this study support the mitochondrial based classification hypothesis of *E*.

marmorata (Spinks and Shaffer 2005; Spinks et al. 2010). This is contrary to the original classification of *E. marmorata* (Holland 1992; Seeliger 1945) and lends credence to the idea that at least some aspect of cryptic diversity is a product of sample size, methodology, or both.

The lack of coherent geographical subclass assignment from PAM clustering (Fig. 4) as well as the large number of features necessary before no increase in AUC for all models (Fig. 6) indicates that the morphological variation between classes is extremely fine grained. This was also exemplified by the small differences between mean class shapes of the final chosen classification scheme (Fig. 11).

The approaches presented here for supervised learning analysis of the landmark variation represent a compromise between explicitly modeling all shape variation and preventing models from being overfit and ungeneralizable. While all aspects of shape may be evolving simultaneously, and not along individual PCs, including all shape variation in each model might increase model complexity beyond a reasonable level for the sample size and possibly the necessary complexity to accurately model the response. Additionally, because only individual PCs are used as features in the models, this does not accurately represent shape evolution and how exactly different classes might be evolving in relation to each other. However, this compromise is not without its advantages. Because both AICc and AUC values improved rapidly with increased model complexity (Fig. 6), this helped demonstrate how fine scale the actual variation between classes was. The variable importance information from the random forest models was extremely useful for understanding what aspects shape variance contributed most to differentiating the classes and in what order as opposed purely in the order of largest variance (Fig. 10 and 11). Additionally, the relative risk values from the multinomial logistic regression models demonstrate that a single PC is probably not sufficient for estimating the class of an observation, but that given a set of PCs this classification would be more accurate (Fig. 12).

454 Ultimately, it would be useful to not require such explicit classification hypotheses,
especially when concerned about possible cryptic variation in extinct taxa. The only unsuper-
456 vised method employed in this study, PAM, is rather simple and not model based. A more
useful approach would be to employ various model based clustering approaches (Fraley and
458 Raftery 2002; Zhong and Ghosh 2003). In this manner, a series of candidate models can be
compared via model comparison methods, such as AIC or Bayes factors (Fraley and Raftery
460 2002), in order to assess the best clustering solution. Here we focused on the results and utility
of supervised methods because they are both more powerful and hypothesis driven (Hastie
462 et al. 2009). Because there are two alternative classification schemes for *E. marmorata*, it was
most appropriate to compare these two hypotheses and estimate which one most accurately
464 reflected the variation. Future work would be to explore and derive unsupervised methods
which corroborate these results.

466 In this study we have demonstrated that, using alternative methodology to that
which is most frequently applied, it is possible to determine which classification scheme best
468 matches variation in a taxon amongst a set of alternative hypotheses. The observed plastral
variation of *E. marmorata* is most consistent with the mitochondrial based hypothesis of
470 Spinks and Shaffer (2005) and Spinks et al. (2010) and not with the original morphology based
hypothesis of Holland (1992); Seeliger (1945). We have also demonstrated the utility of various
472 machine learning approaches to understanding the structure of variation in morphometric
data. Specifically, methods for better understanding misclassification and identifying which is
474 the most important for delimiting different classes. These methods represent new applications
which may be important for future studies on class-based morphological comparison and
476 variation, both in the context of cryptic diversity and with known classifications.

ACKNOWLEDGEMENTS

478 PDS would like to thank David Bapst, Michael Foote, Benjamin Frable, and Dallas Krentzel

for useful discussion which enhanced the quality of this study. For access to emydine specimens,
 480 we thank: J. Vindum and R. Drewes (CAS); A. Resetar (FMNH); R. Feeney (LACM); C.
 Austin (LSUMNS); S. Sweet (MSE); J. McGuire and C. Conroy (MVZ); A. Wynn (NMNH);
 482 P. Collins (SBMNH); B. Hollingsworth (SDMNH); C. Bell and R. Burroughs (TMM); T.
 LaDuc and R. Burroughs (TNHC); P. Holroyd (UCMP); R. Symonds (UMZC); J. Buskirk.
 484 We are grateful to S. Sweet for field assistance and the California Department of Fish and
 Game for permits. Much of the data collection was funded by NSD DBI-0306158 (to KDA).

486 *

References

488 Akaike, H. 1974. A new look at the statistical model identification. *IEEE Transactions on*
Automatic Control 19:716–723.

490 Angielczyk, K. D. and C. R. Feldman. 2013. Are diminutive turtles miniaturized? The ontogeny
 of plastron shape in emydine turtles. *Biological Journal of the Linnean Society* 108:727–755.

492 Angielczyk, K. D., C. R. Feldman, and G. R. Miller. 2011. Adaptive evolution of plastron shape
 in emydine turtles. *Evolution* 65:377–394.

494 Angielczyk, K. D. and H. D. Sheets. 2007. Investigation of simulated tectonic deformation in
 fossils using geometric morphometrics. *Paleobiology* 33:125–148.

496 Breiman, L. 2001. Random Forests. *Machine Learning* 45:5–32.

Breiman, L., J. Friedman, C. J. Stone, and R. A. Olshen. 1984. *Classification and regression*
 498 *trees*. Wadsworth International Group, Belmont.

Burnham, K. P. and D. R. Anderson. 2002. *Model selection and multi-model inference: a*
 500 *practical information-theoretic approach*. 2nd ed. Springer, New York.

- Caumul, R. and P. D. Polly. 2005. Phylogenetic and environmental components of morphological
502 variation: skull, mandible, and molar shape in marmots (*Marmota*, Rodentia). *Evolution;*
international journal of organic evolution 59:2460–72.
- 504 Clare, E. L. 2011. Cryptic species? Patterns of maternal and paternal gene flow in eight
neotropical bats. *PloS one* 6:e21460.
- 506 Demandt, M. H. and S. Bergek. 2009. Identification of cyprinid hybrids by using geometric
morphometrics and microsatellites. *Journal of Applied Ichthyology* 25:695–701.
- 508 Dryden, I. L. 2013. shapes: Statistical shape analysis. R package version 1.1-8.
- Dryden, I. L. and K. Y. Mardia. 1998. Statistical shape analysis. Wiley, New York.
- 510 Eldredge, N. and S. J. Gould. 1972. Punctuated equilibria: an alternative to phyletic gradualism.
Pages 82–115 *in* *Models in Paleobiology* (T. J. M. Schopf, ed.). Freeman Cooper, San
512 Francisco.
- Fraley, C. and A. E. Raftery. 2002. Model-Based Clustering, Discriminant Analysis, and Density
514 Estimation. *Journal of the American Statistical Association* 97:611–631.
- Fujita, M. K., A. D. Leaché, F. T. Burbrink, J. a. McGuire, and C. Moritz. 2012. Coalescent-based
516 species delimitation in an integrative taxonomy. *Trends in ecology & evolution* 27:480–8.
- Funk, W. C., M. Caminer, and S. R. Ron. 2012. High levels of cryptic species diversity uncovered
518 in Amazonian frogs. *Proceedings of the Royal Society B: Biological Sciences* 279:1806–14.
- Gaubert, P., P. J. Taylor, C. a. Fernandes, M. W. Bruford, and G. Veron. 2005. Patterns
520 of cryptic hybridization revealed using an integrative approach: a case study on genetids
(*Carnivora*, *Viverridae*, *Genetta* spp.) from the southern African subregion. *Biological Journal*
522 *of the Linnean Society* 86:11–33.

- Germano, D. J. and G. B. Rathbun. 2008. Growth, population structure, and reproduction of
524 western pond turtles (*Actinemys marmorata*) on the Central Coast of California. *Chelonian
Conservation and Biology* 7:188–194.
- 526 Gould, S. J. and N. Eldredge. 1977. Punctuated equilibria: the tempo and mode of evolution
reconsidered. *Paleobiology* 3:115–151.
- 528 Gündüz, I., M. Jaarola, C. Tez, C. Yenyurt, P. D. Polly, and J. B. Searle. 2007. Multigenic
and morphometric differentiation of ground squirrels (*Spermophilus*, *Scuiridae*, *Rodentia*) in
530 Turkey, with a description of a new species. *Molecular phylogenetics and evolution* 43:916–35.
- Hand, D. J. and R. J. Till. 2001. A Simple Generalisation of the Area Under the ROC Curve
532 for Multiple Class Classification Problems. *Machine Learning* 45:171–186.
- Hastie, T., R. Tibshirani, and J. Friedman. 2009. The elements of statistical learning: data
534 mining, inference, and prediction. 2nd ed. Springer, New York.
- Holland, D. C. 1992. Level and pattern in morphological variation: a phylogeographic study
536 of the western pond turtle (*Clemmys marmorata*). Ph.D. thesis University of Southwestern
Louisiana.
- 538 Holm, S. 1979. A simple sequentially rejective multiple test procedure. *Scandinavian Journal of
Statistics* 6:65–70.
- 540 Hunt, G. 2008. Gradual or pulsed evolution: when should punctuational explanations be
preferred? *Paleobiology* 34:360–377.
- 542 Hurvich, C. M. and C.-L. Tsai. 1989. Regression and time series model selection in small
samples. *Biometrika* 76:297–307.
- 544 Kaufman, L. and P. J. Rousseeuw. 1990. Finding groups in data : an introduction to cluster
analysis. Wiley, New York.

- 546 Kendall, D. G. 1977. The diffusion of shape. *Advances in Applied Probability* 9:428–430.
- Kendall, D. G. 1984. Shape Manifolds, Procrustean Metrics, and Complex Projective Spaces.
548 *Bulletin of the London Mathematical Society* 16:81–121.
- Klingenberg, C. P., M. Barluenga, and A. Meyer. 2002. Shape analysis of symetric structures:
550 quantifying variation among individuals and asymmetry. *Evolution* 56:1909–1920.
- Kuhn, M. 2013. caret: Classification and Regression Training. R package version 5.15-61.
- 552 Liaw, A. and M. Wiener. 2002. Classification and regression by randomforest. *R News* 2:18–22.
- Lubcke, G. M. and D. S. Wilson. 2007. Variation in shell morphology of the Western Pond
554 Turtle (*Actinemys marmorata* Baird and Giarard) from three aquativ habitats in Northern
California. *Journal of Herpetology* 41:107–114.
- 556 MacLeod, N. 2007. Automated taxon identification in systematics: theory, approaches and
applications. CRC Press, Boca Raton.
- 558 Maechler, M., P. Rousseeuw, A. Struyf, M. Hubert, and K. Hornik. 2013. cluster: Cluster
Analysis Basics and Extensions. R package version 1.14.4.
- 560 Mitteroecker, P. and F. Bookstein. 2011. Linear Discrimination, Ordination, and the Visualiza-
tion of Selection Gradients in Modern Morphometrics. *Evolutionary Biology* 38:100–114.
- 562 Pfenninger, M. and K. Schwenk. 2007. Cryptic animal species are homogeneously distributed
among taxa and biogeographical regions. *BMC evolutionary biology* 7:121.
- 564 Polly, P. D. 2003. Paleophylogeography of *Sorex araneus*: molar shape as a morphological marker
for fossil shrews. *Mammalia* 68:233–243.
- 566 Polly, P. D. 2007. Phylogeographic differentiation in *Sorex araneus*: morphology in relation to
geography and karyotype. *Russian Journal of Theriology* 6:73–84.

- 568 R Core Team. 2013. R: A Language and Environment for Statistical Computing. R Foundation
for Statistical Computing Vienna, Austria.
- 570 Rohlf, F. J. 2005. TpsDig 2.04.
- Seeliger, L. M. 1945. Variation in the Pacific Mud Turtle. *Copeia* 1945:150–159.
- 572 Spinks, P. Q. and H. B. Shaffer. 2005. Range-wide molecular analysis of the western pond
turtle (*Emys marmorata*): cryptic variation, isolation by distance, and their conservation
574 implications. *Molecular ecology* 14:2047–64.
- Spinks, P. Q., R. C. Thomson, and H. B. Shaffer. 2010. Nuclear gene phylogeography reveals
576 the historical legacy of an ancient inland sea on lineages of the western pond turtle, *Emys*
marmorata in California. *Molecular ecology* 19:542–56.
- 578 Stuart, B. L., R. F. Inger, and H. K. Voris. 2006. High level of cryptic species diversity revealed
by sympatric lineages of Southeast Asian forest frogs. *Biology letters* 2:470–4.
- 580 Tibshirani, R., G. Walther, and T. Hastie. 2001. Estimating the number of clusters in a
data set via the gap statistic. *Journal of the Royal Statistical Society: Series B (Statistical*
582 *Methodology)* 63:411–423.
- Venables, W. and B. D. Ripley. 2002. *Modern applied statistics with S*. 4th ed. Springer, New
584 York.
- Yang, Z. and B. Rannala. 2010. Bayesian species delimitation using multilocus sequence data.
586 *Proceedings of the National Academy of Sciences* 107:9264–9.
- Zelditch, M. L., D. L. Swiderski, and H. D. Sheets. 2004. *Geometric morphometrics for biologists:*
588 *a primer*. Elsevier Academic Press, Amsterdam.

Zhong, S. and J. Ghosh. 2003. A unified framework for model-based clustering. The Journal of
590 Machine Learning Research 4:1001–1037.

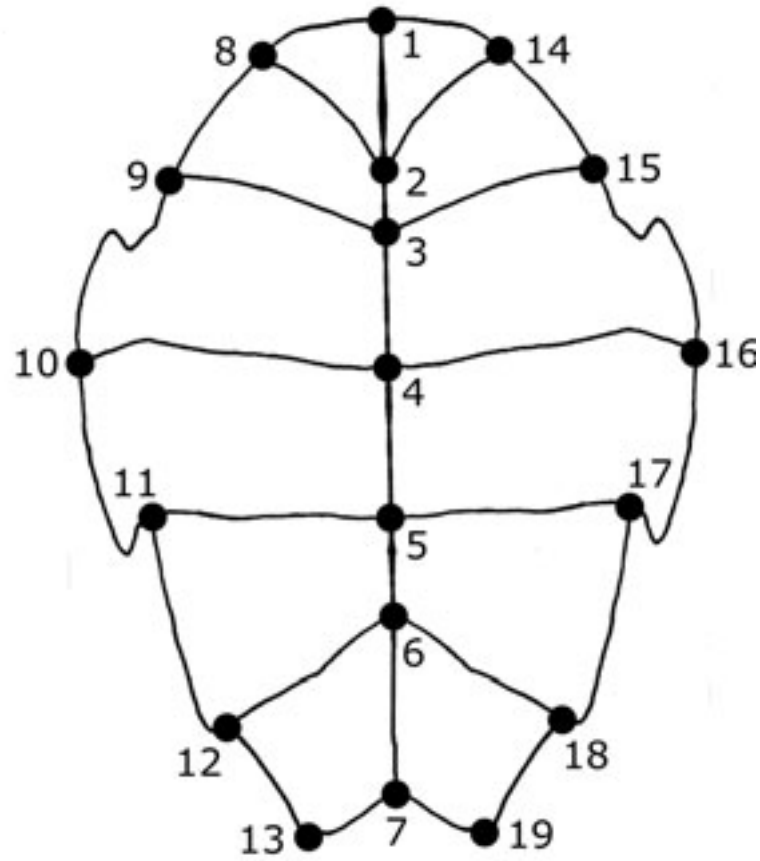


Figure 1: Depiction of general plastral shape of *E. marmorata* and position of the 19 landmark used in this study. Anterior is towards the top of the figure.

		Predicted class	
		1	0
Actual class	1	TRUE POSITIVE	FALSE NEGATIVE
	0	FALSE POSITIVE	TRUE NEGATIVE

Table 1: Example confusion matrix. The columns correspond to the predicted class of an observation, while the rows correspond to the actual class of that observation. Depending on the type match between the prediction and reality, four different outcomes are possible: true positive (TP), false negative (FN), false positive (FP), and true negative (TN). These four quantities are used for calculating all confusion matrix statistics. Each of these values is an integer and the sum of the number of occurrences of that event during classification.

	F	M	tot
1	101	112	213
2	99	87	186
tot	200	199	399

Table 2: Tabular comparison between sex observation and cluster assignment from PAM with two clusters. This number of clusters was chosen because it represented the second best clustering solution as determined via gap statistic comparison (Fig. 4). χ^2 analysis of this contingency table showed that there is no relationship between sex observation and cluster assignment (χ^2 : 1.12, df: 1, p -value: 0.29).

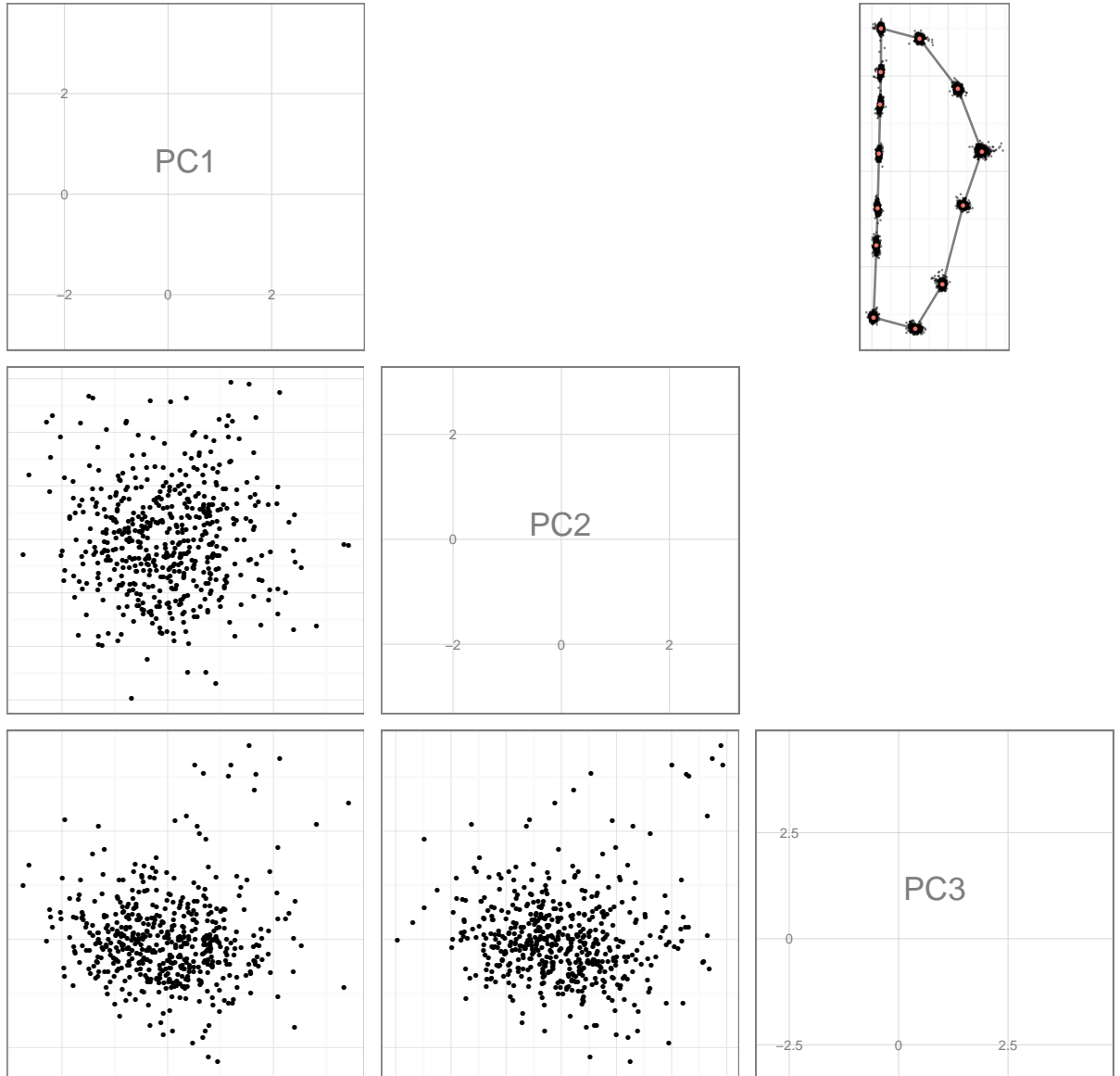


Figure 2: Results from PCA of the Procrustes superimposed “half” plastral landmarks. Depicted here are the for three PCs (lower triangle) and the mean shape with observed variance around each point (upper right). The first three PCs account for total 45.2924805932624% of the variance in plastral shape.

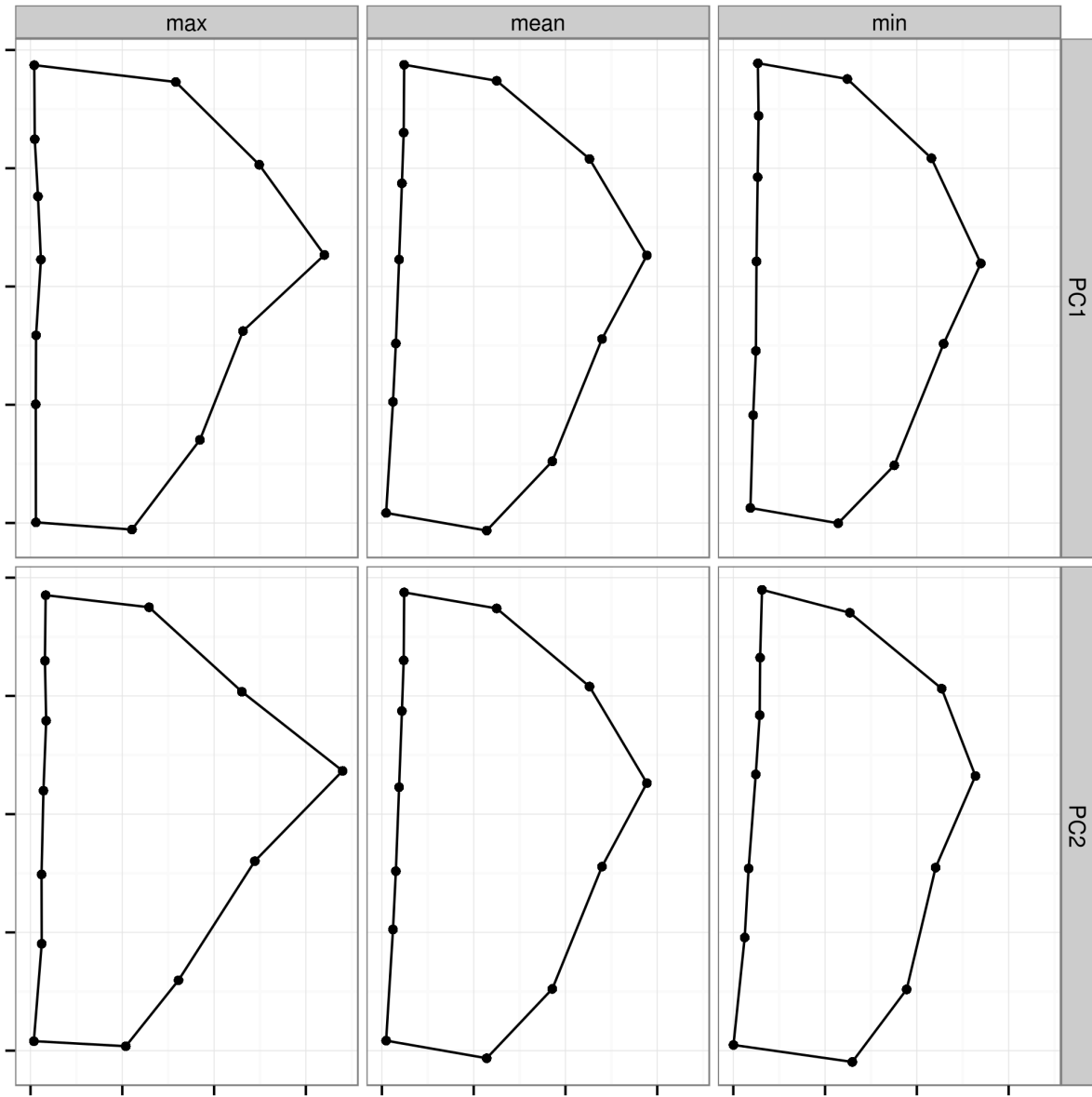


Figure 3: Landmark variation along the first two PCs of the Procrustes superimposed “half” plastral landmarks. The first row corresponds to variation along the first PC, while the second row corresponds to the second PC. The left most column represents the observation with the highest eigenscore along that PC, while the right most column represents the observation with the lowest eigenscore. The middle column, for both rows, is the mean plastral shape for all observations. The first PC represents 20.32% of the total variation in plastral shape while PC represents 12.78% of the variance.

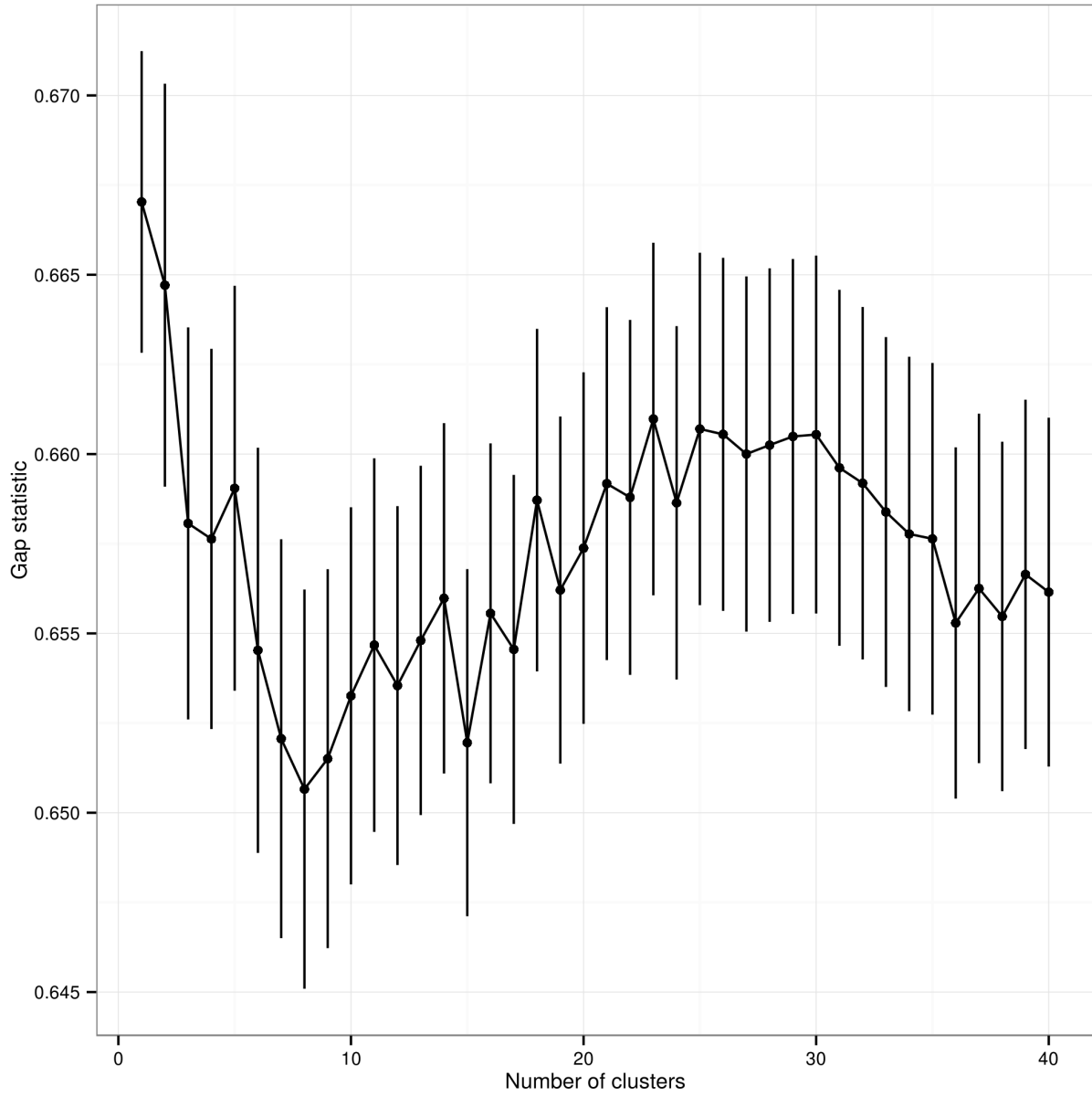


Figure 4: Gap statistic values for PAM clustering results for the ρ dissimilarity matrix of plastron shape. Error bars are standard errors estimated via 500 bootstrap samples.

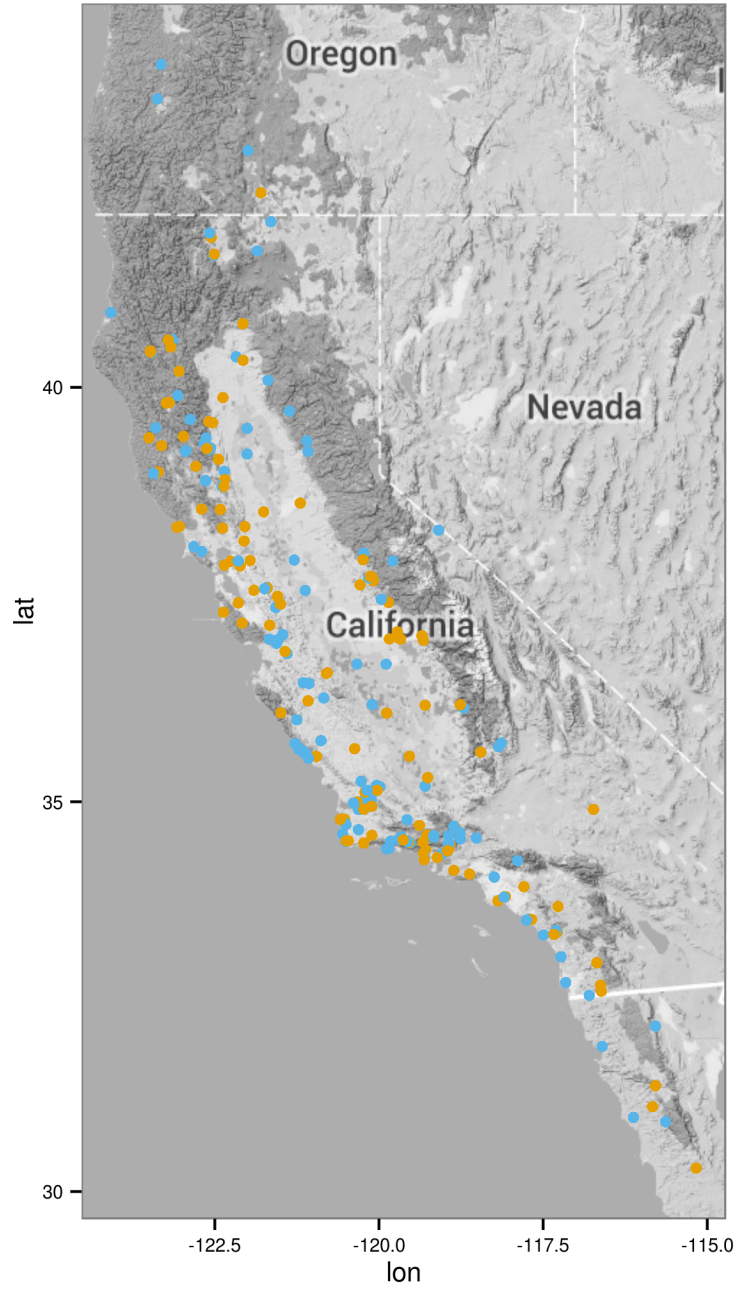


Figure 5: Clustering solution for PAM with two medoids for the entire set of observed *E. marmorata*. Clustering was based entirely on the ρ dissimilarity matrix of “half” plastral landmark configurations following Procrustes superimposition.

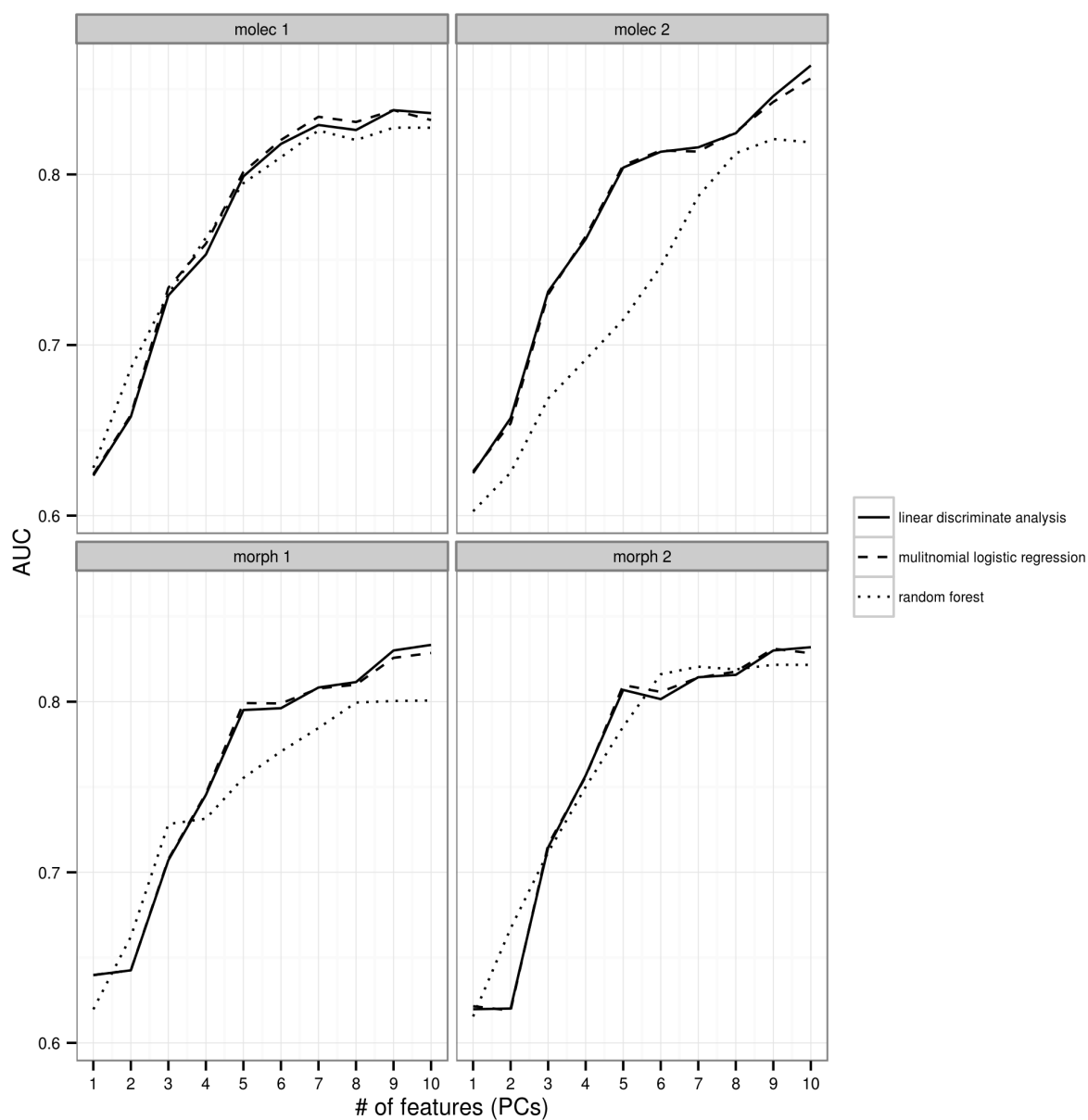


Figure 6: Effect of increasing the number of PCs as features, or predictors, of classification of plastra for all four classification schemes. As the total number of features increase, AUC increases until eventually leveling off. Both multinomial logistic regression and random forest models are illustrated here, though AUC based model selection was only performed for random forest models.

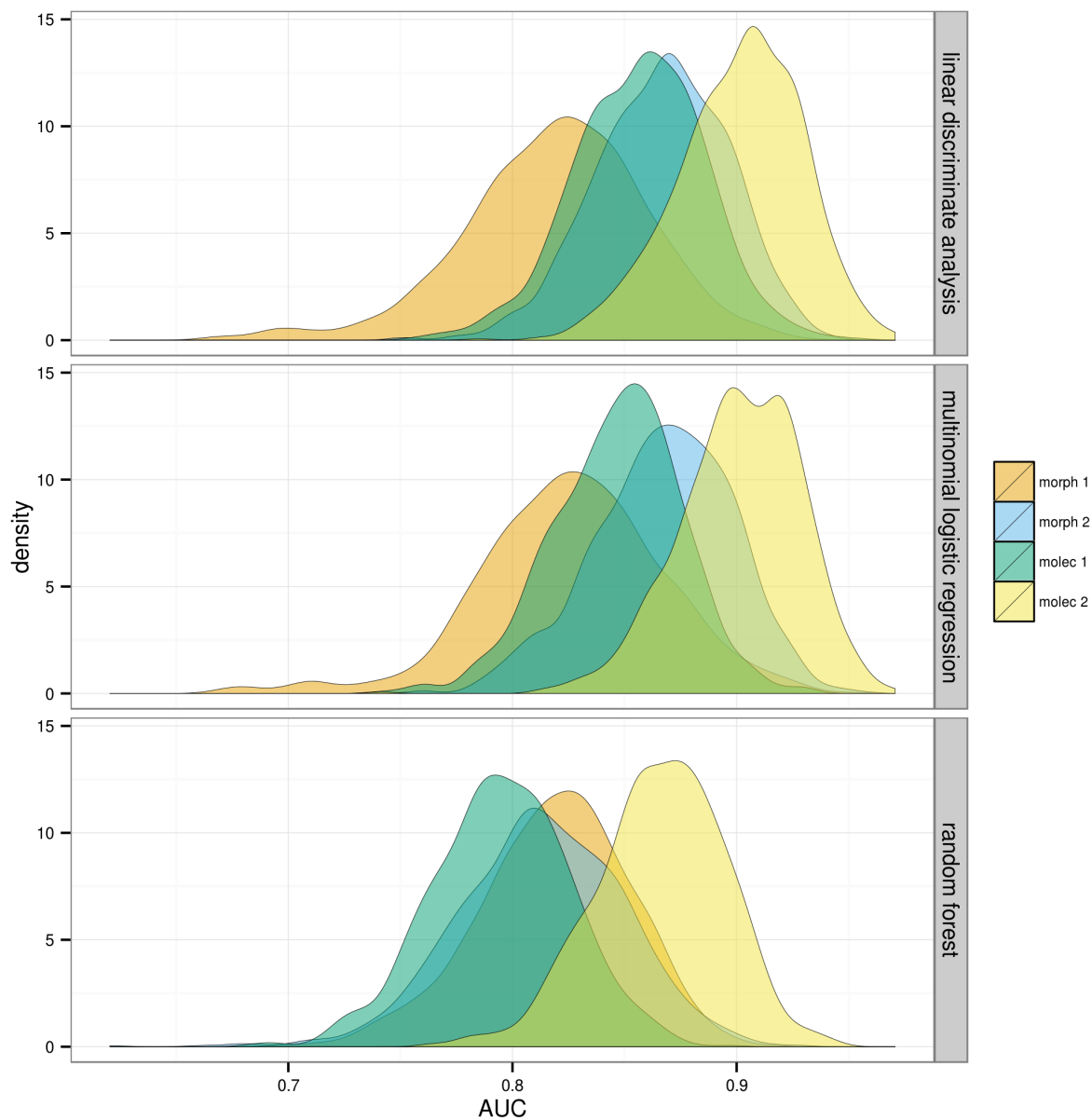


Figure 7: Density estimates of AUC values of predictions of the testing dataset of plastra from 1000 bootstrap resamples. The top facet corresponds to values using the optimal multinomial logistic regression model, as chosen by minimum AICc value. The bottom facet corresponds to the values using the optimal random forest model, as chosen by maximum AUC value.

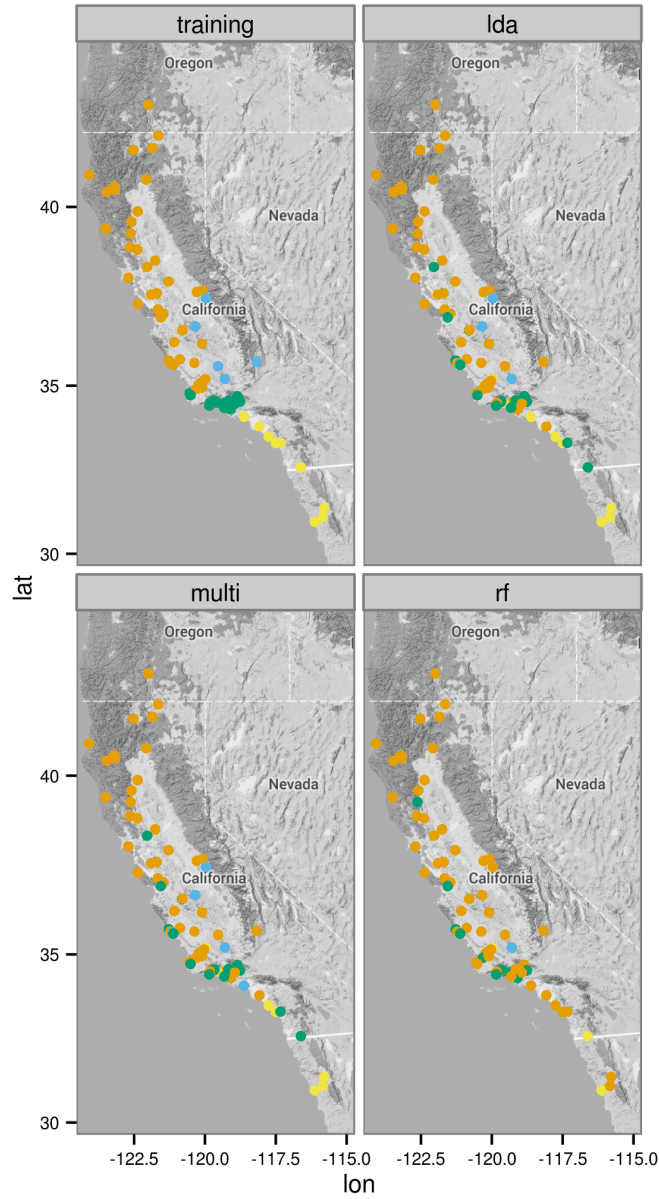
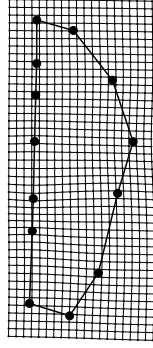
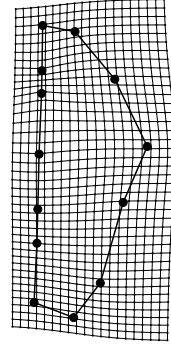


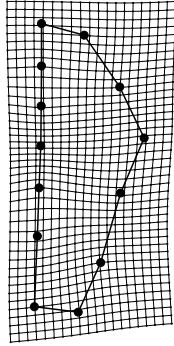
Figure 8: Comparison between reference classification of testing data set and the estimated classifications based on the selected multinomial logistic regression and random forest models, from left to right respectively. Classification corresponds to the four classes as suggested by the hypothesis of Spinks and Shaffer (2005) and Spinks et al. (2010).



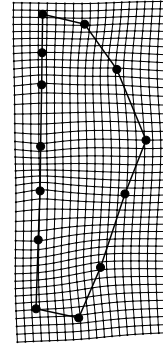
(a) Northern



(b) Eastern



(c) Western



(d) Southern

Figure 9: Thin-plate splines for each of the four classes from the best classification hypothesis based on the generalization results (Fig. 7). The four different classes are labeled according to the biogeographic groups as depicted in figure 8. The deformations are depicted with 2x magnification from base.

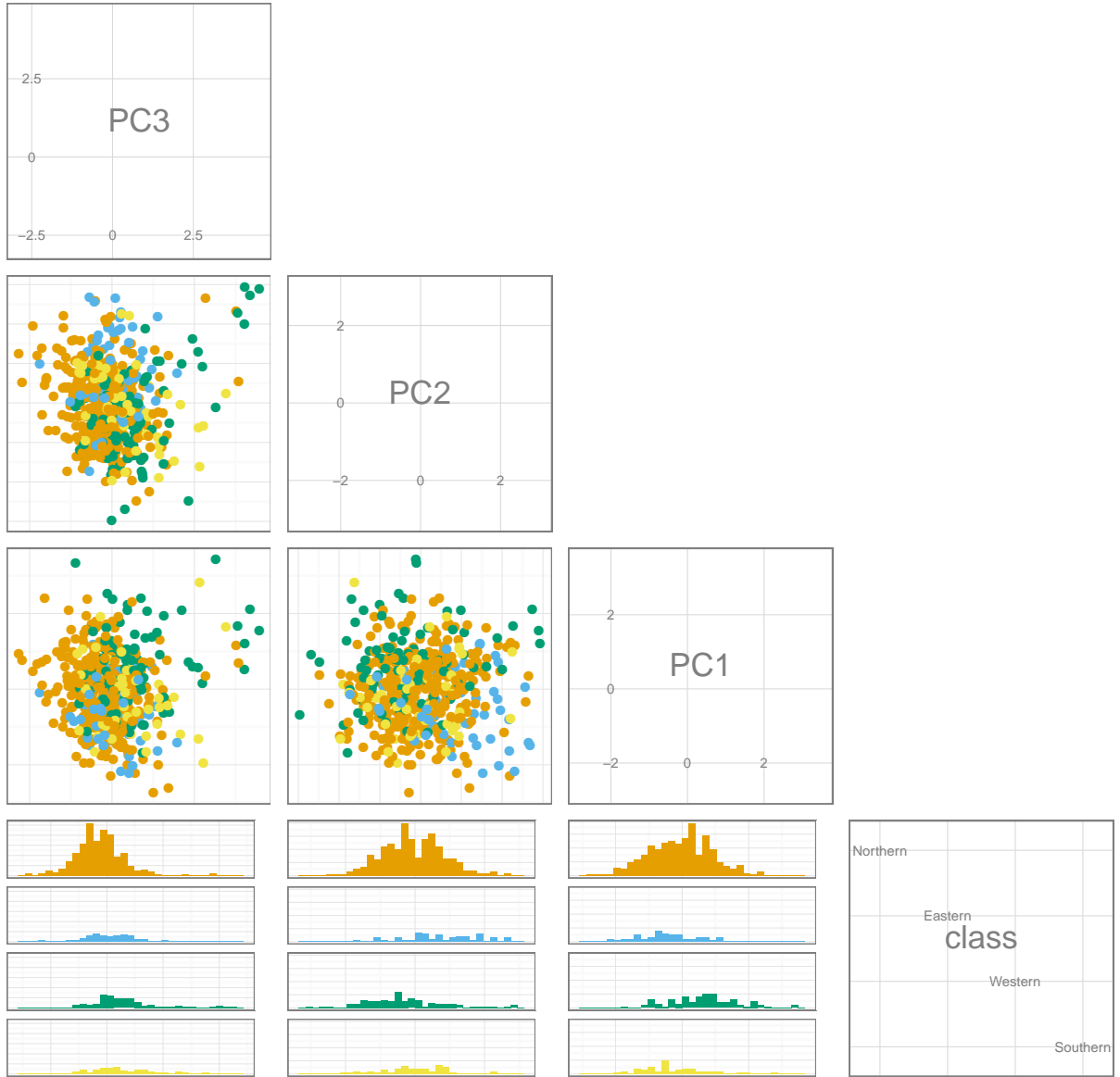


Figure 10: Pairs plot of the first three most important variables of the optimal random forest model of turtle plastral shape. The variables descend in importance from the upper left to the lower right. The observations are colored as in figure 8. The bottom row are histograms of classification occurrences along the PCs.

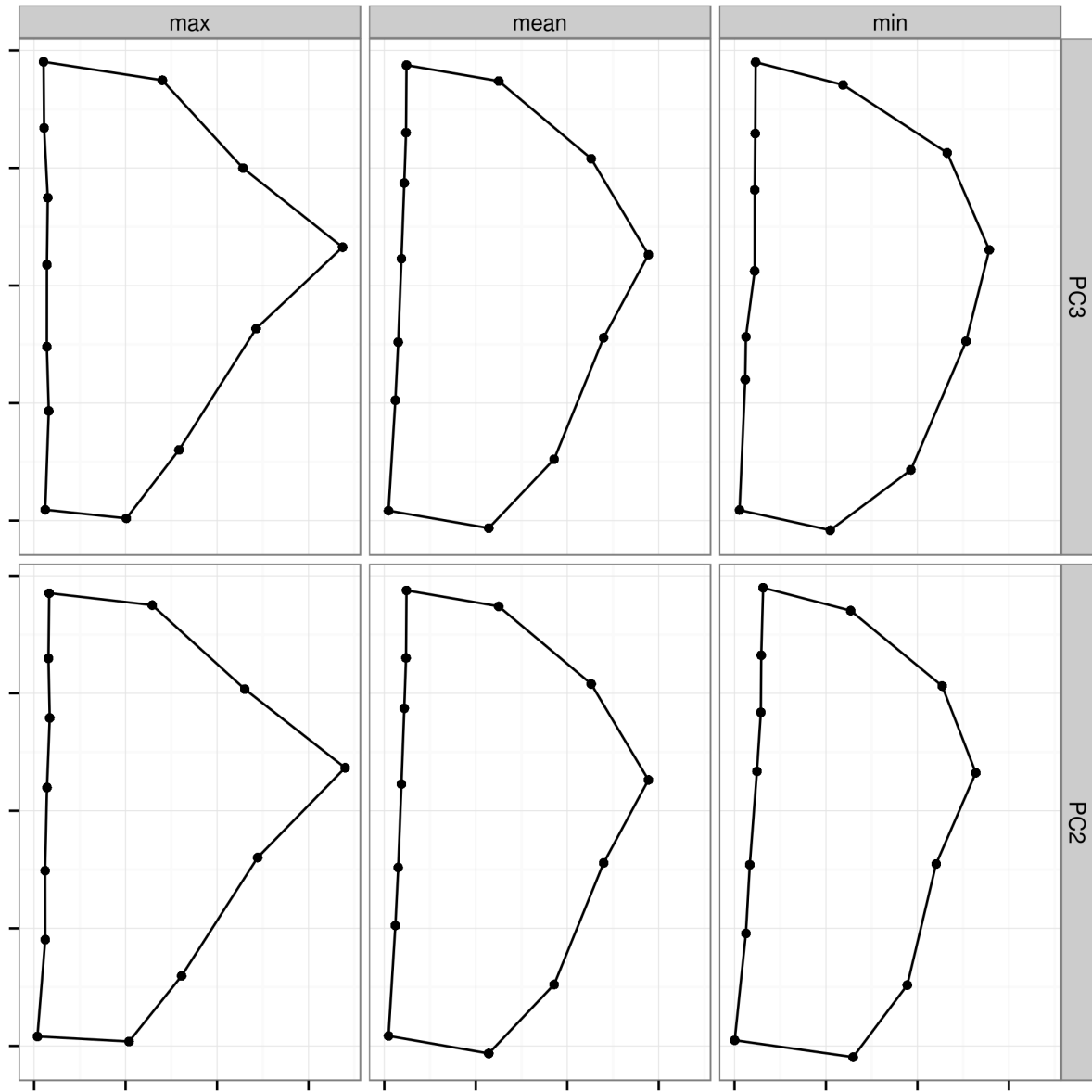


Figure 11: Landmark variation along the two most important features (PCs) based on the final random forest model. The first row corresponds to the third PC and the second corresponds to the second PC. Landmark configurations are minimum observed on that PC, mean shape, and maximum observed on that PC.

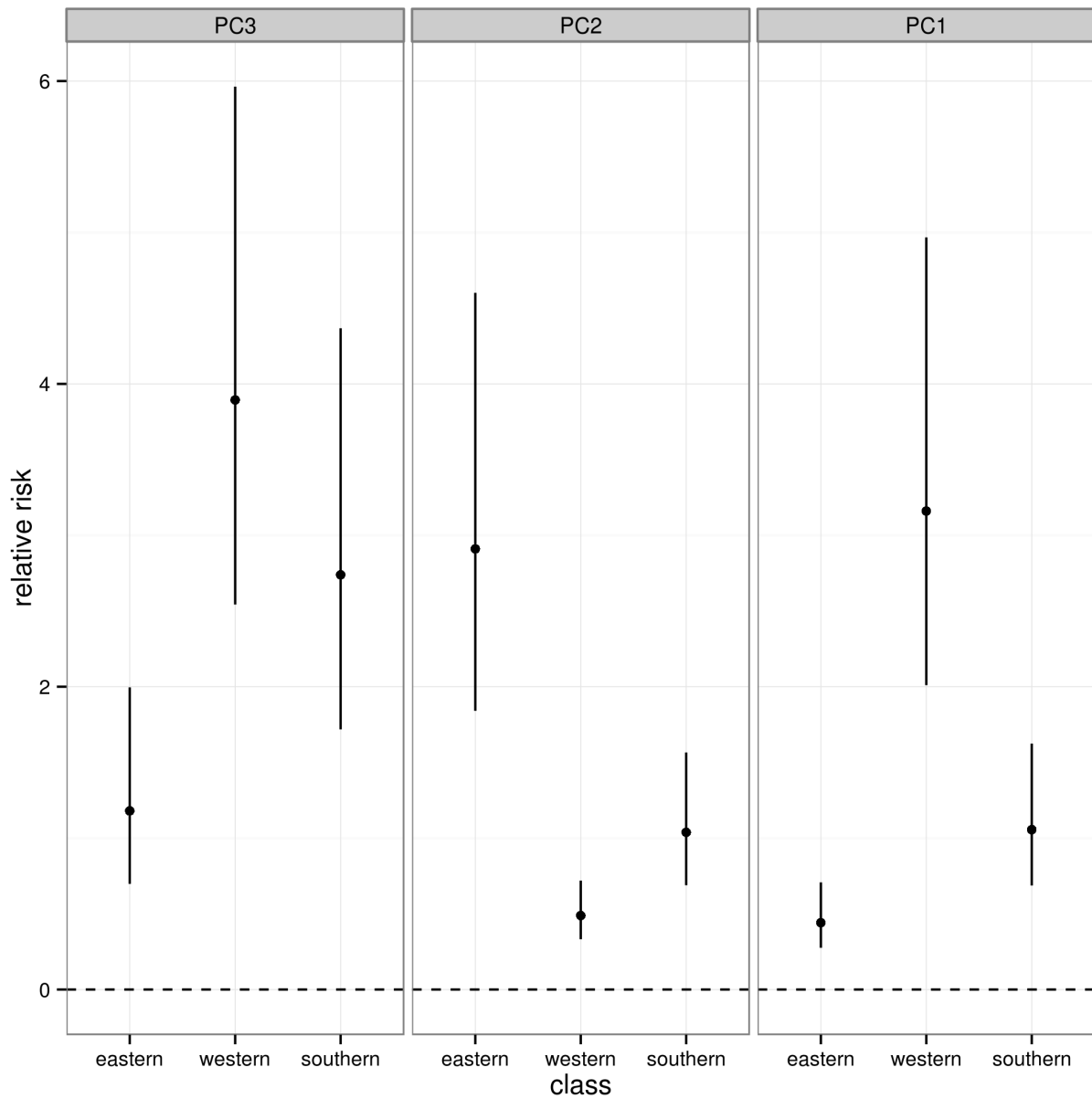


Figure 12: Forest plot of the relative risk, with 95% confidence intervals, of classifying a give specimen based on the first three most important variables according to the random forest model. Relative risk values are calculated from the coefficients of the multinomial logistic regression model. All risks are relative to the northern group from Spinks and Shaffer (2005); Spinks et al. (2010). Variable importance is from left to right.

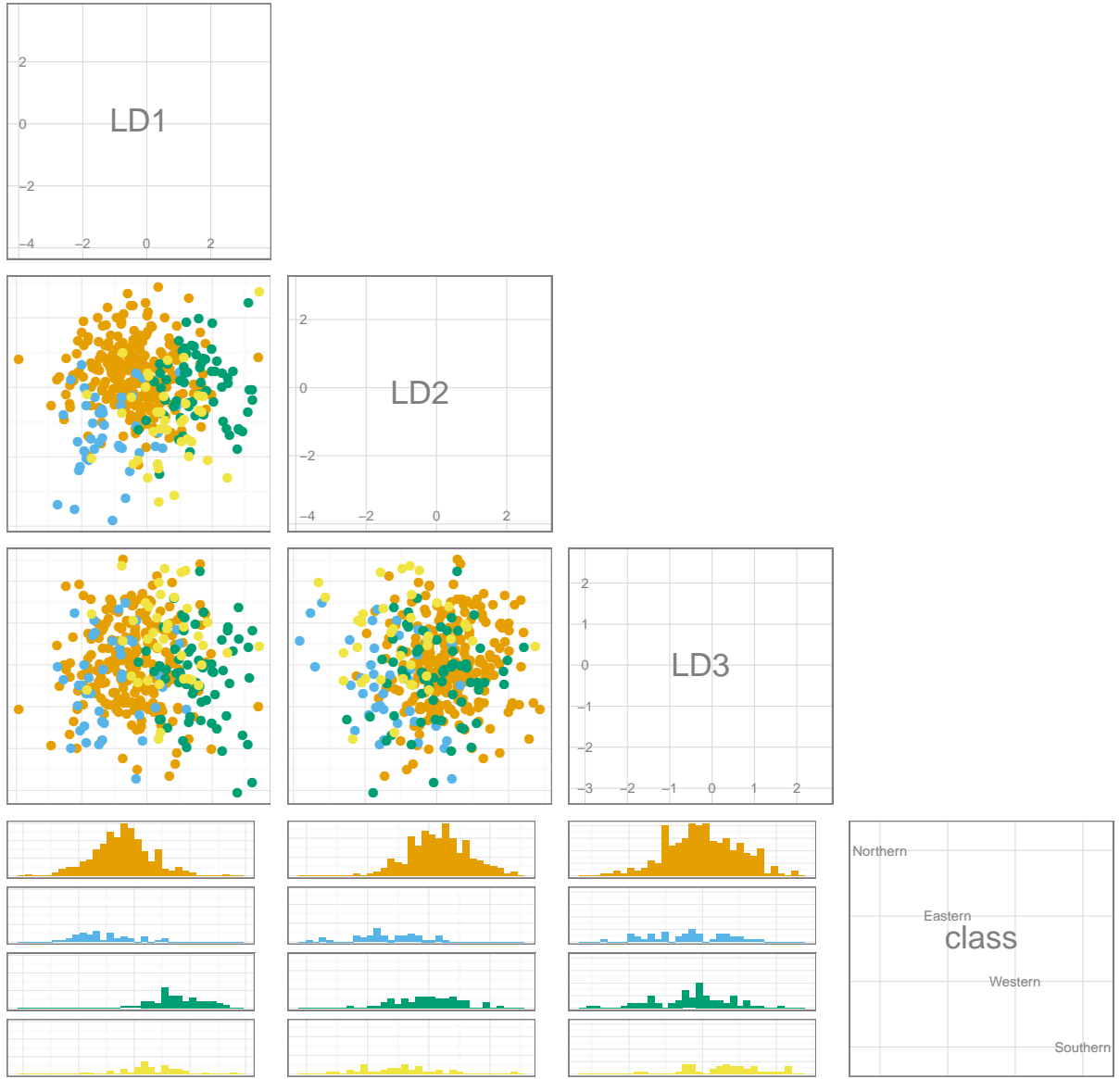


Figure 13: Pairs plots of the three discriminate axes from the linear discriminate analysis of the eigenscores from the first 10 PCs of plastral shape. The observations figured are from from the training data set used for all models for the second molecular classification hypothesis based on Spinks and Shaffer (2005) and Spinks et al. (2010). Observations are colored as in Fig. 8.

(Intercept)	PC1	PC2	PC3	PC4	PC5	PC6	PC7	PC8	PC9	PC10	df	logLik	AICc	delta	weight
+	+	+	+	+	+	+	+	+	+		20.00	-250.00	542.26	0.00	0.64
+	+	+	+	+	+	+	+	+	+	+	22.00	-248.35	543.43	1.18	0.36
+	+	+	+	+	+	+	+				16.00	-261.94	557.33	15.07	0.00
+	+	+	+	+	+	+	+	+			18.00	-259.99	557.82	15.56	0.00
+	+	+	+	+	+	+					14.00	-275.68	580.48	38.22	0.00
+	+	+	+	+							12.00	-281.10	587.03	44.77	0.00
+	+	+	+	+							10.00	-305.55	631.68	89.43	0.00
+	+	+	+								8.00	-318.48	653.34	111.09	0.00
+	+										6.00	-344.14	700.49	158.24	0.00
+											4.00	-346.80	701.71	159.45	0.00

Table 3: Model selection table for the multinomial logistic regression models of the first morphologically based classification hypothesis. This classification hypothesis corresponds to “morph 1” also depicted in figures 6 and 7. This hypothesis is based on Seeliger (1945). The column “delta” corresponds to the δAICc values of each model, while “weights” correspond to the Akaike weight of that model relative to all others.

(Intercept)	PC1	PC2	PC3	PC4	PC5	PC6	PC7	PC8	PC9	PC10	df	logLik	AICc	delta	weight
+	+	+	+	+	+	+	+	+	+		20.00	-245.15	532.56	0.00	0.83
+	+	+	+	+	+	+	+	+	+	+	22.00	-244.53	535.79	3.23	0.17
+	+	+	+	+	+	+	+	+			18.00	-254.69	547.21	14.64	0.00
+	+	+	+	+	+	+					16.00	-258.00	549.45	16.88	0.00
+	+	+	+	+	+	+					14.00	-268.69	566.49	33.93	0.00
+	+	+	+	+	+						12.00	-271.30	567.42	34.86	0.00
+	+	+	+	+							10.00	-298.53	617.64	85.07	0.00
+	+	+	+								8.00	-314.50	645.37	112.81	0.00
+	+	+									6.00	-342.94	698.10	165.53	0.00
+	+										4.00	-349.55	707.20	174.64	0.00

Table 4: Model selection table for the multinomial logistic regression models of the first morphologically based classification hypothesis. This classification hypothesis corresponds to “morph 2” also depicted in figures 6 and 7. This hypothesis is based on Seeliger (1945). The column “delta” corresponds to the $\delta AICc$ values of each model, while “weights” correspond to the Akaike weight of that model relative to all others.

(Intercept)	PC1	PC2	PC3	PC4	PC5	PC6	PC7	PC8	PC9	PC10	df	logLik	AICc	delta	weight
+	+	+	+	+	+	+	+	+	+		30.00	-303.61	672.34	0.00	0.77
+	+	+	+	+	+	+	+	+	+	+	33.00	-301.25	674.74	2.41	0.23
+	+	+	+	+	+	+	+	+			27.00	-314.28	686.70	14.36	0.00
+	+	+	+	+	+	+					24.00	-318.22	687.70	15.37	0.00
+	+	+	+	+	+	+					21.00	-335.11	714.71	42.37	0.00
+	+	+	+	+	+						18.00	-353.04	743.91	71.57	0.00
+	+	+	+	+							15.00	-385.20	801.67	129.34	0.00
+	+	+	+								12.00	-397.69	820.21	147.87	0.00
+	+										9.00	-437.13	892.73	220.39	0.00
+	+										6.00	-451.19	914.60	242.27	0.00

Table 5: Model selection table for the multinomial logistic regression models of the first morphologically based classification hypothesis. This classification hypothesis corresponds to “molec 1” also depicted in figures 6 and 7. This hypothesis is based on Seeliger (1945). The column “delta” corresponds to the δAICc values of each model, while “weights” correspond to the Akaike weight of that model relative to all others.

(Intercept)	PC1	PC2	PC3	PC4	PC5	PC6	PC7	PC8	PC9	PC10	df	logLik	AICc	delta	weight
+	+	+	+	+	+	+	+	+	+	+	33.00	-251.73	575.67	0.00	1.00
+	+	+	+	+	+	+	+	+	+		30.00	-268.54	602.18	26.51	0.00
+	+	+	+	+	+	+	+	+			27.00	-283.99	626.10	50.43	0.00
+	+	+	+	+	+	+					24.00	-295.61	642.46	66.78	0.00
+	+	+	+	+	+	+					21.00	-302.50	649.48	73.81	0.00
+	+	+	+	+	+						18.00	-316.59	671.00	95.32	0.00
+	+	+	+	+							15.00	-340.84	712.95	137.27	0.00
+	+	+	+								12.00	-353.01	730.84	155.17	0.00
+	+										9.00	-378.16	774.78	199.11	0.00
+											6.00	-395.71	803.64	227.97	0.00

Table 6: Model selection table for the multinomial logistic regression models of the first morphologically based classification hypothesis. This classification hypothesis corresponds to “molec 2” also depicted in figures 6 and 7. This hypothesis is based on Seeliger (1945). The column “delta” corresponds to the $\delta AICc$ values of each model, while “weights” correspond to the Akaike weight of that model relative to all others.

	morph 1	morph 2	molec 1	molec 2
morph 1				
morph 2	0.00			
molec 1	0.00	0.00		
molec 2	0.00	0.00	0.00	

Table 7: Results from pairwise Mann-Whitney U test between the AUC distributions of the generalizations of the multinomial logistic regression models. Labels correspond to those in Figure 7. Values of 0 correspond to p-values lower than 0.01. P-values were corrected for multiple comparison using the Holm method (Holm 1979).

	morph 1	morph 2	molec 1	molec 2
morph 1				
morph 2	0.00			
molec 1	0.00	0.00		
molec 2	0.00	0.00	0.00	

Table 8: Results from pairwise Mann-Whitney U test between the AUC distributions of the generalizations of the random forest models. Labels correspond to those in Figure 7. Values of 0 correspond to p-values lower than 0.01. P-values were corrected for multiple comparison using the Holm method (Holm 1979).

	morph 1	morph 2	molec 1	molec 2
morph 1				
morph 2	0.00			
molec 1	0.00	0.00		
molec 2	0.00	0.00	0.00	

Table 9: Results from pairwise Mann-Whitney U test between the AUC distributions of the generalizations of the LDA-based classification from the first 10 PCs of plastral shape. Labels correspond to those in Figure 7. Values of 0 correspond to p-values lower than 0.01. P-values were corrected for multiple comparison using the Holm method (Holm 1979).